Inorganica Chimica Acta, 203 (1993) 43–49

Hydrogen migration in $Fe_3(CO)_9CH_4$

Annette R. Howells and Maria C. Milletti*
Department of Chemistry, Eastern Michigan University, Ypsilanti, MI 48197 (USA)

(Received May 27, 1992; revised August 21, 1992)

Abstract

The Fenske–Hall method of semi-empirical molecular orbital calculations was used to analyze the capped transition metal cluster $Fe_3(CO)_9CH_4$. This type of cluster is of interest because it can be used as a model for the activation of hydrocarbons on metal surface catalysts. The process of hydrogen migration between the metal base and the cap was studied, with particular emphasis on the agostic M–C–H interaction, which occurs in some isomers of the compound. For the three isomers produced in the migration process, the primary distinction that leads to the variation in stabilities among these structures is the extent of metal–metal overlap between 3d orbitals of the iron atoms. It was found that, if there are hydrogen atoms bridging the metal centers at the base of the complex, the isomer is stabilized by the reduction of overlap between atomic orbitals on adjacent metal centers, thereby reducing the impact of filled metal–metal antibonding orbitals. Agostic interactions between cap hydrogens and the base also tend to stabilize the compound. This was found to be largely due to a reorganization of the bond between the carbon in the capping group and the agostic metals. In addition, Mulliken overlap populations indicate that the hydrogens involved in M–C–H agostic interactions also reduce metal–metal overlap.

Introduction

The principal purpose of this project was to study the process of hydrogen migration that occurs in the capped transition metal cluster, $Fe_3(CO)_9CH_4$. The Fenske–Hall method of approximate molecular orbital calculations [1] was used to analyze the bonding in the compound, which exists as a mixture of isomers in equilibrium (see Fig. 1). Metal clusters of this type are useful as models of catalytic metal surfaces. This particular compound is especially interesting because of the presence, in some isomers, of agostic bonds between metal atoms and hydrogen atoms on the capping group. Agostic bonding is a relatively new concept and is not yet thoroughly understood [2]. Consequently, a second objective of the project was to explore the nature of agostic bonding, both in terms of the orbital interactions involved and the stabilizing effect it produces.

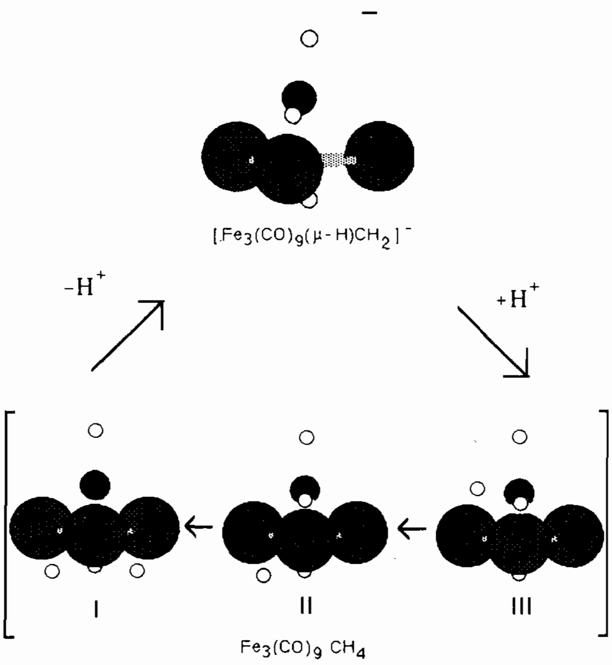

Fig. 1. Structure of $[Fe_3(CO)_9(\mu\text{-}H)CH_2]^-$ and of the isomers of $Fe_3(CO)_9CH_4$. Each large sphere represents a $Fe(CO)_3$ moiety; black spheres are carbon atoms, and white spheres are hydrogen atoms.

The migration process under consideration is depicted in Fig. 1. Physical evidence of this process comes from NMR spectral data gathered on both the isomers in equilibrium and the related anionic compound, $[Fe_3(CO)_9CH_3]^-$ [3, 4]. The anion is formed by the deprotonation of structure I at room temperature [3]. During this reaction, one of the hydrogens in the metal–metal bridging positions is removed and it is believed that a second one migrates to form a bridge between a metal atom and the carbon atom of the capping group [4]. This carbon–hydrogen–metal bridge

---

*Author to whom correspondence should be addressed.

0020-1693/93/$6.00

can be considered an agostic interaction. As the anion is protonated at low temperature (−70 °C), an isomer of $Fe_3(CO)_9CH_4$ is formed, which contains multiple agostic interactions (structure III). This is the kinetic product of the reaction, but not the thermodynamic product, since hydrogens migrate from the cap to bridging positions between the metal atoms as the solution is heated (structures II and I). At room temperature the dominant isomer is structure I, the thermodynamic product. The first phase of this work was the analysis of the three isomers of $Fe_3(CO)_9CH_4$ in terms of their structure and relative energies and the determination of the causes of the variation in stabilities between the isomeric configurations.

The second phase of research involved analysis of the agostic bonding detected in some of the isomers of the complex. 'Agostic' is a term first coined in 1983 by Brookhart and Green [5]. It describes an asymmetric hydrogen bridge between a transition metal and a non-metal. While the hydrogen is covalently bonded to the non-metal, a bonding interaction can be detected between the metal and the hydrogen atom. Often this interaction manifests itself as a geometrical distortion of the structure that brings the hydrogen of a C–H bond closer to the transition metal. For example, in $Fe_3(CO)_9(\mu\text{-}H)CH_3$, structure III, the agostic distortion involves the rotation of the methyl cap towards the metal triangle, as depicted in Fig. 1. In a study of the hypothetical complexes $H_5TiCH_3^{-2}$ and H_3TiCH_3, Eisenstein and Jean have suggested that reorganization of the carbon metal bond, as the geometry of the molecule is distorted, provides the major stabilizing influence in agostic interactions [6]. The current study was an opportunity to test this hypothesis on a set of compounds which are more complex than the idealized titanium compounds.

Details of the calculations

The results of this study were obtained by conducting a series of Fenske–Hall calculations, which were performed on a VAX mainframe computer, model 118650. The atomic basis set that was used consisted of Slater double zeta functions taken from the set derived by Clementi [7]. The zeta exponent for the hydrogen 1s function was set at 1.6, a value which generates the minimum energy in calculations for methane [8]. Fe 4s and 4p orbitals were constructed by maximizing overlap with the carbon atom from a carbonyl ligand [8]. The zeta exponent for both the 4s and 4p orbitals was set at 1.68.

Since no X-ray structures were available for the complexes of interest, a set of X-ray diffraction data for the compound $H_3Fe_3(CO)_9CCH_3$ [9] was used as a starting point. This data provided the coordinates used for the metal triangle, carbonyl ligands and bridging hydrogens in all of the isomers studied. Other bond distances and angles in the complexes, such as those for the R group capping the metal triangle, were optimized by carrying out a series of calculations with slight changes in the geometry. For isomers containing agostic interactions, initial estimates of agostic bonding distances between the carbon and hydrogen on the cap and the respective Fe centers were based on known values [10]. Both the total Hartree–Fock energy [11] and the energy gap between the highest occupied molecular orbital (HOMO) and the lowest unoccupied molecular orbital (LUMO) in the molecule were used as criteria to determine the best geometry.

The geometric parameters that were optimized in the various configurations are shown in Fig. 2. In the Figure, the double agostic conformation of $Fe_3(CO)_9(\mu\text{-}H)CH_3$ (structure III) serves as a model for identifying these parameters. They include L, the distance between the cap carbon and the center of the metal triangle; l, the C–H bond length for an agostic hydrogen, and θ, the M–C–H agostic angle. Other variables include the angle of the carbonyl ligands with respect to the metal triangle plane, ϕ, the position of non-agostic hydrogens, and the inclusion of a bridging hydrogen between specific pairs of metal atoms. This last set of parameters was not optimized in all isomers, but only in a few. The coordinates for the metal bridging hydrogens were kept the same as those in the $Fe_3(CO)_9CCH_3$ structure, although the number of bridging hydrogens in each isomer may vary.

For the double agostic conformation of structure III, several techniques were employed to model the dual agostic interaction. The method that produced the lowest energy values was to point the agostic hydrogens directly at the corresponding metal atoms, while varying the M–C–H angle and cap-to-base distance. An issue that surfaced when analyzing the geometries of structures II and III was the placement of the bridging hydrogens. The coordinates of these hydrogens were

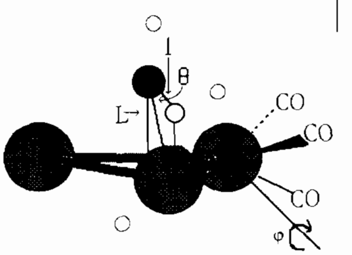

Fig. 2. Geometric parameters optimized in most of the isomers, illustrated on structure **III**.

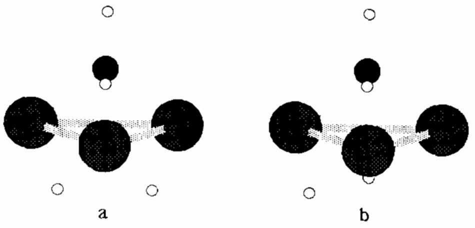

Fig. 3. Symmetric and asymmetric isomers of $Fe_3(CO)_9(\mu\text{-}H)_2CH_2$. The asymmetric configuration shown in (b) is energetically favored.

made to match coordinates from the original X-ray data, but which two metal atoms the hydrogen bridges were varied in order to study the effect on the stability of the complex. Optimization calculations were performed for the double agostic conformation of structure II with the lone bridging hydrogen placed between the two agostic interacting metals. This conformation is shown in Fig. 3(a). The results indicate that this placement is energetically unfavorable. No set of parameters could be found for this symmetric configuration which produced a more favorable structure than the optimized geometry determined for the asymmetric conformation, shown in Fig. 3(b). Likewise, for the $Fe_3(CO)_9(\mu\text{-}H)_2CH_2$ isomer, the favored position of the bridging hydrogens was the asymmetric placement similar to that in Fig. 3(b). The significance of these results is discussed below.

Results and discussion

The analysis of the compounds of interest was approached from two perspectives. The first was to consider the energetics of the migration of hydrogen between the cap and the metal base. The second point of interest was to investigate the nature of the C–H–M agostic interaction in terms of the molecular orbitals involved.

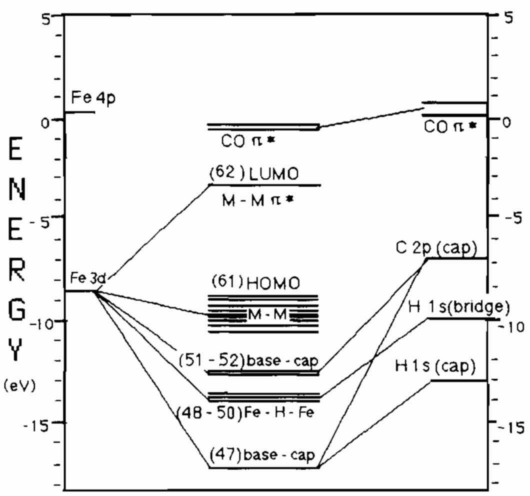

Fig. 4. Molecular orbital diagram for $Fe_3(CO)_9(\mu\text{-}H)_3CH$. Thick lines represent two or more molecular orbitals.

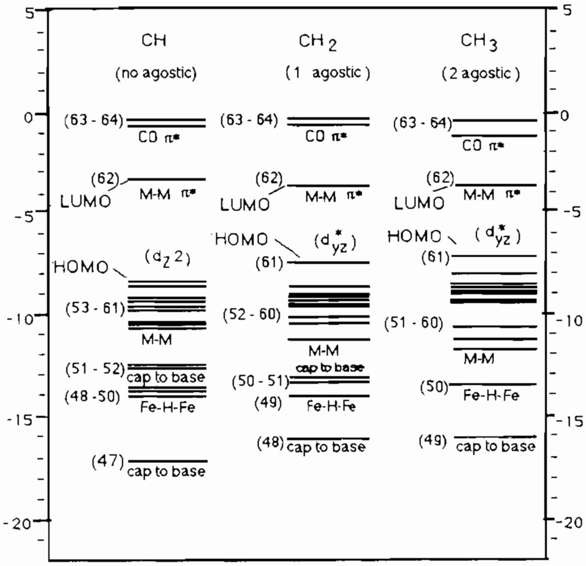

Fig. 5. Comparative molecular orbital diagram for the three isomers of $Fe_3(CO)_9CH_4$. Thick lines represent two or more molecular orbitals.

The theoretical analysis of the migration process in the $Fe_3(CO)_9CH_4$ cluster was carried out by performing calculations on the three isomers found in equilibrium in solution. Figure 4 is the molecular orbital diagram for the alkylidyne isomer. Analysis of the diagram reveals a pattern of molecular orbitals that is also present in the other isomers. The three orbitals representing the bridging interaction between hydrogen and iron atoms at the base of the cluster appear at low energies. These three bridging orbitals are formed by overlap between the hydrogen 1s atomic orbitals and $3d_{yz}$ and $3d_{xz}$ orbitals from the adjacent metal atoms. Akylidyne cap-to-metal base bonding occurs in orbitals 47, 51 and 52, as shown in Fig. 4. In orbitals 51 and 52 the carbon $2p_x$ and $2p_y$ orbitals form π bonds with metal d orbitals of corresponding symmetry. In orbital 47, carbon $2p_z$ and 2s orbitals interact primarily with the cap hydrogen. However, they are also appropriately aligned to form a σ bond with the d_{z^2} orbitals on the iron centers. A band of orbitals at higher energy represents both bonding and antibonding interactions between metal centers. This band includes the highest occupied molecular orbital (HOMO) and the lowest unoccupied molecular orbital (LUMO).

Molecular orbital diagrams were also obtained for the alkylidene and alkyl capped isomers. Diagrams for all three molecules are presented in Fig. 5, where some differences among isomers can be observed. First of all, as a hydrogen migrates from the base and bonds to the cap, a cap-to-base interaction disappears. This can be seen by comparing the number of cap-to-base orbitals for each isomer in Fig. 5, which decreases from three (47, 51, 52) to two (48, 51) to one (49) going from left to right. The carbon $2p_x$ and $2p_y$ orbitals contributing to the molecular orbitals of $Fe_3(CO)_9(\mu\text{-}H)_3CH$ are directed to bonding with the added hydrogens on the cap in $Fe_3(CO)_9(\mu\text{-}H)_2CH_2$ and $Fe_3(CO)_9(\mu\text{-}H)CH_3$. In contrast to that rearrangement, the overlap between cap hydrogens and the carbon $2p_z$ and 2s orbitals decreases. As more hydrogens are added to the cap, a stronger σ bond develops between these carbon orbitals and the metal d_{z^2} orbitals. This interaction occurs in molecular orbitals 48 and 49 of the $Fe_3(CO)_9(\mu\text{-}H)_2CH_2$ isomer and the $Fe_3(CO)_9(\mu\text{-}H)CH_3$ isomer, respectively. Another change that occurs as hydrogens migrate to the cap involves the hydrogen-metal bridging orbitals. Bonding with the bridge hydrogens occurs in orbitals 48–50 in the alkylidyne structure, where the metal atoms use d_{yz} and d_{xz} orbitals to bond with the bridging hydrogens. Figure 5 shows that, as each bridging hydrogen is removed, a M–H–M bonding orbital disappears. A final distinction among the diagrams worth noting is that the metal–metal overlap band spreads out as hydrogens are removed from bridging positions. This reduces the size of the HOMO – LUMO gap and consequently the stability of the molecule. It therefore appears that the molecule is destabilized as hydrogens move from the base to the cap. Mulliken overlap populations [12] presented in Table 1 show an increase in metal–metal overlap as hydrogens are removed from the base. Because of the antibonding character of the higher-energy M–M orbitals, the increase in overlap pushes these molecular orbitals to higher energies, thus reducing the HOMO – LUMO gap and creating a destabilizing effect.

More specifically, in the alkylidyne isomer the metal d orbitals bonding with the bridging Hs are d_{yz} and d_{xz} and, as hydrogens are removed, the d_{yz} orbitals are left to bond with each other. The extent of M–M π overlap is then increased, the amount of d_{yz} character in the antibonding orbitals of the M–M band is also increased and the orbitals are pushed up in energy. This causes the $d_{yz}{}^*$ orbital to become the HOMO and decreases the HOMO – LUMO gap, which diminishes the stability of the complex. Table 2 presents the values of the calculated total energy and the HOMO – LUMO energy gap for the three isomers. These data indicate that the alkylidyne structure is the most stable of the three isomers, both in terms of total energy and HOMO – LUMO gap. These results corroborate what is depicted in Fig. 5 and detected by NMR spectrometry. Similar conclusions have also been reached using *ab initio* techniques on the hypothetical isolobal main-group cluster model $H_3(BH)_3CCH_3$ [13].

TABLE 1. Mulliken overlap populations[a] for the metal 3d orbitals of the three $Fe_3(CO)_9CH_4$ isomers

$Fe_3(CO)_9(\mu\text{-}H)_3CH$	$Fe_3(CO)_9(\mu\text{-}H)_2CH_2$	$Fe_3(CO)_9(\mu\text{-}H)CH_3$
0.061	0.063	0.091

[a]Overlap populations listed are the sum of all overlap populations between metal orbitals for each molecule.

TABLE 2. Total energy[a] and HOMO – LUMO gap for the three $Fe_3(CO)_9CH_4$ isomers

Isomer	Total energy	HOMO – LUMO gap
$Fe_3(CO)_9(\mu\text{-}H)_3CH$	−741	5.57
$Fe_3(CO)_9(\mu\text{-}H)_2CH_2$	−730	3.85
$Fe_3(CO)_9(\mu\text{-}H)CH_3$	−716	3.43

[a]Total energy values are relative and should be used only comparatively.

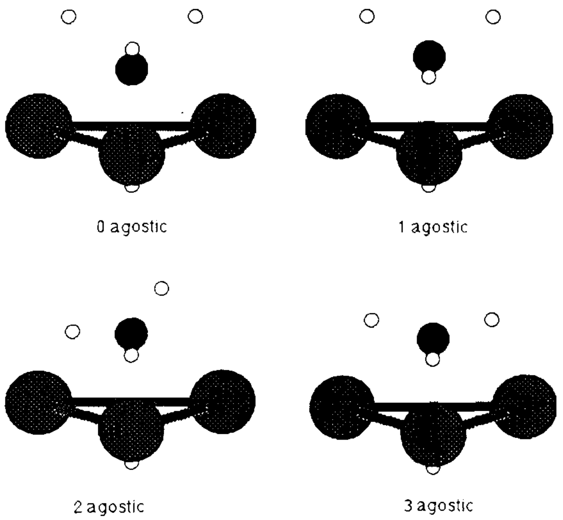

0 agostic

1 agostic

2 agostic

3 agostic

Fig. 6. Possible conformations of $Fe_3(CO)_9(\mu\text{-}H)CH_3$, showing between zero and three agostic interactions.

The methyl capped cluster, $Fe_3(CO)_9(\mu\text{-}H)CH_3$, was selected as the focus of the second part of this study, since this molecule can be envisioned as having between zero and three agostic interactions, as shown in Fig. 6. By studying the four isomers in Fig. 6, the effect of adding and removing agostic bonds from a particular compound can be studied. Molecular orbital calculations were carried out on each of the four possible isomers of $Fe_3(CO)_9(\mu\text{-}H)CH_3$ to determine which one had the lowest energy. Figs 7 and 8 present comparisons of the molecular orbital diagrams for all $Fe_3(CO)_9(\mu\text{-}H)(CH_3)$ structures. Due to the complexity and relatively low symmetry of this compound, mixing of the molecular orbitals is extensive and it is difficult to isolate specific orbitals that depict cap-to-metal interactions. In order to clarify certain aspects of the bonding picture in this complex, Fig. 8 shows selected molecular orbitals from the M–M band depicted in Fig. 7. These particular orbitals were singled out because they best illustrate the cap-to-base bonding interactions of interest.

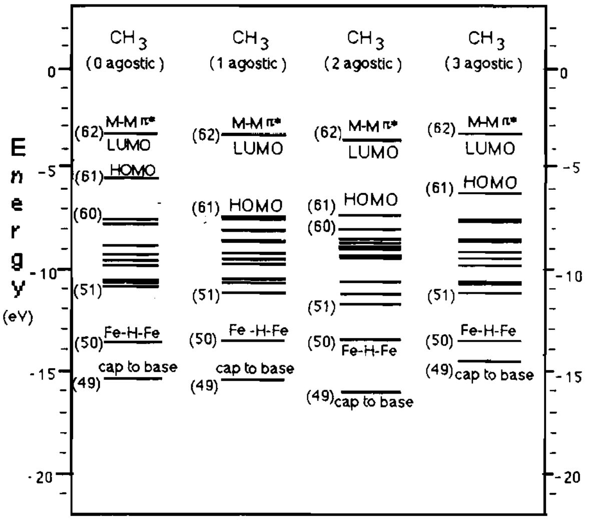

Fig. 7. Comparative molecular orbital diagram for the four conformations of $Fe_3(CO)_9(\mu\text{-}H)CH_3$. Thick lines represent two or more molecular orbitals.

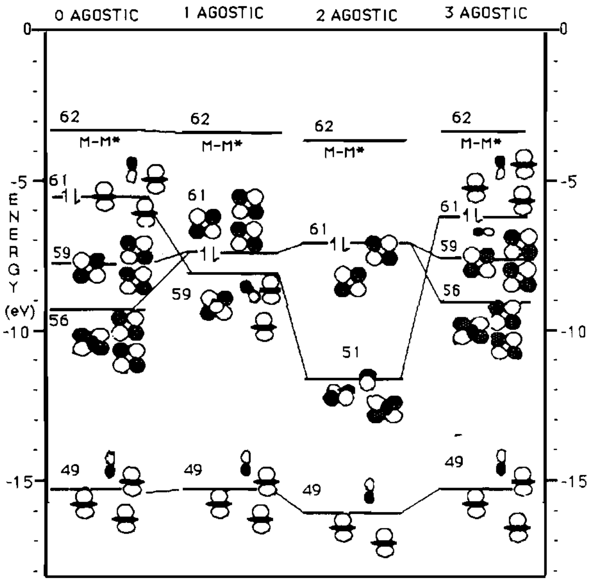

Fig. 8. Comparative molecular orbital diagram for the four conformations of $Fe_3(CO)_9(\mu\text{-}H)CH_3$ showing selected orbitals.

The nature of this part of the analysis was to trace changes that occur in specific orbitals as the geometry of $Fe_3(CO)_9(\mu\text{-}H)CH_3$ changes. Figure 8 best depicts changes occurring in the bonding between the cap carbon and metal centers. In the conformation with no agostic hydrogens, the orbitals with the largest metal-to-cap bonding character are 49 and 61, the latter being the HOMO of the complex. In both of these orbitals the $C2p_z$ orbital overlaps primarily with the $3d_{z^2}$ orbitals of the metal atoms. As previously mentioned, carbon $2p_x$ and $2p_y$ orbitals are mainly occupied in bonding to the cap hydrogens.

Orbital 49 maintains approximately the same energy in all four isomers. However, a more interesting picture is obtained as one traces the higher energy cap contribution in orbital 61 through the isomers, as the cap is tilted toward one or more of the metal centers. As one agostic interaction is formed, the d_{z^2} orbital on the agostic metal hybridizes with the d_{yz} orbital in order to better overlap with the cap. This interaction appears in orbital 59 of the single agostic conformation and it is at a lower energy than the orbital 61 it originates from. The $C2p_z$ orbital, though mixed with a small $C2p_y$ contribution, still maintains a σ interaction with the three metal centers. At the same time, two orbitals with d_{yz} character, orbitals 56 and 59 in the zero agostic conformation, combine to form the HOMO, orbital 61, in the single agostic structure. Because this orbital occurs at a lower energy than the HOMO in the zero agostic structure, the rearrangement of the orbitals leads to a widening of the HOMO – LUMO gap.

Moving from the single to the double agostic structure, the cap-to-base interaction has moved to an even lower energy (orbital 51) and it consists of the $C2p_x$ orbital σ bonding to one of the agostic metals. Using a d_{yz} orbital, the other agostic iron now forms a π bond to the $C2p_x$ orbital. The HOMO appears fairly similar in form and energy to the HOMO for the single agostic conformation. In the triple agostic structure, a certain degree of symmetry is regained and the molecular orbital diagram for this structure bears a striking similarity to the diagram of the zero agostic conformation. Again the HOMO is a cap-to-base interaction between the $C2p_z$ and the unhybridized Fe d_{z^2} atomic orbitals. Likewise, the metal–metal π interaction occurs in orbitals 56 and 59, at roughly the same energy as in the zero agostic structure.

Table 3 presents the total energies and HOMO – LUMO gap energies for the four $Fe_3(CO)_9(\mu\text{-}H)CH_3$ conformations. This set of data shows that the reorganization of the cap-to-base interaction, first in the single and then in the double agostic isomer, corresponds to a progressive lowering of the total energy of the structure. Also, the HOMO – LUMO gap is larger in the single and double agostic isomers than in the zero and triple agostic isomers. These factors,

TABLE 3. Total energy[a] and HOMO – LUMO gap for the four isomers of $Fe_3(CO)_9(\mu\text{-}H)CH_3$

Isomer	Total energy	HOMO – LUMO gap
Zero agostic	−692	2.21
One agostic	−702	3.97
Two agostic	−716	3.43
Three agostic	−708	2.83

[a] Total energy values are relative and should be used only comparatively.

of course, imply an increase of stability in the single and, especially, the double agostic isomers. In conclusion, it appears that the stabilization associated with agostic bonding is mainly the result of the reorganization of the bonds between the cap carbon and metal triangle, which occurs as the geometric orientation of the capping group changes.

The conclusion stated above differs somewhat from the more obvious explanation that agostic bonding simply consists of a charge donation from a hydrogen atom or C–H bond to an electron deficient metal. In this work, hydrogen atoms were not found to contribute significantly to orbitals containing large cap carbon and metal contributions. Furthermore, no three centered, C–H–M bonding orbital was found in any of the agostic conformations, although such an orbital represents an obvious interpretation of an agostic bond. Some overlap between the hydrogen 1s, carbon 2s, and iron 4s atomic orbitals was present at low energies, but the metal 4s orbitals are known to be rather diffuse and their overlap with other centers is usually of little significance.

On the other hand, the results of this study do not completely discount the influence of hydrogen–metal overlap in agostic interactions, either. For instance, evidence of the importance of donation of charge to the metal can be found in the optimization results presented earlier. One example is that a stable structure could not be attained for the symmetric isomer in Fig. 3(a), where, presumably, the agostic metals are already saturated by electron donation from the bridging hydrogen. Furthermore, the most stable configuration for the $Fe_3(CO)_9(\mu\text{-}H)CH_3$ triple agostic isomer was attained when the M–H distance was made shorter between the metal isolated from the bridging hydrogen and the corresponding agostic hydrogen than the M–H distance in the remaining agostic metal–hydrogen pairs. This shows that charge contribution from a bridging hydrogen reduces the inclination of a metal to undergo agostic interaction.

The most compelling evidence of the influence of hydrogen charge donation on the stability of the complex is derived from the analysis of the Mulliken overlap populations in Table 4. The data show that the agostic hydrogens in $Fe_3(CO)_9(\mu\text{-}H)CH_3$ isomers fulfill a function similar to that of the metal bridging hydrogens in the series of isomers shown in Fig. 1. The trend seen in Table 4 is that, as agostic bonds form, the metal–agostic hydrogen overlap populations increase and the metal–metal overlap populations decrease. Bonding between an agostic hydrogen and a metal diverts the d orbitals of the metal from interacting with other metals, just as a bond formed with metal–metal bridging hydrogen does. For the series of isomers in Fig. 1, the reduction in metal–metal overlap leads to an increase in stability. The reduction in M–M overlap and corresponding increase in H–M overlap in the agostic isomers correlates to an increase in stability as well.

TABLE 4. Mulliken overlap populations for the four isomers of $Fe_3(CO)_9(\mu\text{-}H)CH_3$

Type of overlap	Zero agostic	One agostic	Two agostic
Metal–metal	0.135	0.128	0.091
Cap H–metal	0.076	0.214	0.353
Cap C–metal	0.230	0.255	0.383

Conclusions

The study of hydrogen migration process in $Fe_3(CO)_9CH_4$ was approached from two perspectives. The first objective was to compare the structures and relative stabilities of the three isomers of the molecule that are in equilibrium. The second objective was to analyze the agostic bonding interactions that occur between cap hydrogens and metals in some of these isomers.

For the three isomers produced in the migration process, the primary distinction that leads to the variation in stabilities among these structures is the extent of metal–metal overlap between 3d orbitals of the iron atoms. Some of the higher-energy molecular orbitals contain enough metal–metal antibonding character that an increase in metal–metal overlap has a net destabilizing effect. This is most clearly seen when comparing molecular orbital diagrams for the three isomers, where it is apparent that, in the less stable structures, there is a dispersion of the band of metal–metal orbitals. This effect is related to the presence or absence of hydrogen atoms in the bridging positions along the metal triangle. When hydrogen atoms are placed in these positions, the metal centers use some of their d orbitals to bond with the hydrogens. Consequently, the presence of more hydrogens in the base bridging positions leads to a decrease in metal–metal overlap populations, which in turn lowers the energy of the highest occupied molecular orbitals and results in an energetically more stable structure. As hydrogens migrate from the base and bond to the cap, the opposite effect is seen. These results are in accord with NMR spectral evidence, which shows the structure with the alkylidyne cap as the most stable.

The structure of $Fe_3(CO)_9(\mu\text{-}H)CH_3$ can be envisioned as containing anywhere from zero to three agostic interactions. All four conformations of this compound were analyzed in order to study the nature of the agostic interaction and, essentially, two effects were found. First of all, a comparison of molecular orbital diagrams obtained for each isomer revealed that, as the number of agostic bonds increases from zero to two, the orbital representing the bond between the cap carbon and metal base is progressively lowered in energy, leaving the structure with two agostic interactions as the most stable one. This is caused by a rehybridization of atomic orbitals on both the carbon and the agostic metal centers. The triple agostic conformation regains some degree of symmetry and, consequently, has the same bonding characteristics as the zero agostic isomer. As a result, this isomer is destabilized.

The second effect observed was that the agostic hydrogens appear to serve a function similar to that of the metal base bridging hydrogens mentioned in the analysis of the migration process. In the conformations of $Fe_3(CO)_9(\mu\text{-}H)CH_3$, the overlap population between the agostic hydrogens and metal 3d orbitals increases as the stability of the isomer increases. Conversely, the removal of agostic bonds corresponds to an increase in the metal–metal overlap population and a decrease in stability.

Acknowledgement

The authors thank Dr José Vites for suggesting the problem and for many helpful discussions.

References

1 R. F. Fenske and M. B. Hall, *Inorg. Chem., 11* (1972) 768.

2 Z. Dawoodi and M. L. H. Green, *J. Chem. Soc., Dalton Trans.,* (1986) 1629.

3 J. C. Vites, T. K. Dutta and T. P. Fehlner, *J. Am. Chem. Soc., 107* (1985) 5563.

4 T. K. Dutta, J. C. Vites, G. B. Jacobsen and T. P. Fehlner, *Organometallics, 6* (1987) 842.

5 M. Brookhart and M. L. H. Green, *J. Organomet. Chem., 250* (1983) 395.

6 O. Eisenstein and Y. Jean, *J. Am. Chem. Soc., 107* (1985) 1177.

7 E. Clementi, *J. Chem. Phys., 40* (1964) 1944.

8 R. F. Fenske, K. G. Caulton, D. D. Radtke and C. C. Sweeney, *Inorg. Chem., 5* (1966) 951.

9 K. S. Wong, K. J. Haller, T. K. Dutta, D. M. Chipman and T. P. Fehlner, *Inorg. Chem., 21* (1982) 3197.

10 F. A. Cotton and G. Wilkinson, *Advanced Inorganic Chemistry,* Wiley, New York, 5th edn., 1988, p. 201.

11 M. C. Milletti and R. F. Fenske, *Organometallics, 8* (1989) 420.

12 W. J. Hehre, L. Radom, P. v. R. Schleyer and J. A. Pople, *Ab Initio Molecular Orbital Theory,* Wiley, New York, 1985, p. 25.

13 M. M. Lynam, D. M. Chipman, R. D. Barreto and T. P. Fehlner, *Organometallics, 6* (1987) 2405.